Available online at www.sciencedirect.com
ScienceDirect
Polymer 48 (2007) 6254–6261
polymer
www.elsevier.com/locate/polymer

Efficient preparation of isotactic polypropylene/montmorillonite nanocomposites by in situ polymerization technique via a combined use of functional surfactant and metallocene catalysis

Kefang Yang[1], Yingjuan Huang, Jin-Yong Dong*

CAS Key Laboratory of Engineering Plastics, Joint Laboratory of Polymer Science and Materials, Institute of Chemistry, Chinese Academy of Sciences, Beijing 100080, China

Received 11 April 2007; received in revised form 31 July 2007; accepted 18 August 2007
Available online 22 August 2007

Abstract

In order to promote efficiency of the preparation of isotactic polypropylene (i-PP)/montmorillonite (MMT) nanocomposites by in situ polymerization technique, a strategy was laid out to enhance both the intercalative selectivity and the catalyst activity of the in situ polymerization by a combined use of a functional surfactant for MMT modification and a metallocene catalyst system for isospecific propylene polymerization. Thus, (2-hydroxylethyl) hexadecyl diethylammonium iodine was involved in the ion-exchanged organic modification of MMT, leading to an implantation of catalyst-anchoring reactive sites (hydroxyl, OH) in the interlayer galleries of MMT (OMMT). By treating the OH-intercalated OMMT successively with excessive methylaluminoxane (MAO) and *rac*-Me_2Si(2-Me-4-Ph-Ind)$_2ZrCl_2$, the metallocene catalyst typical for i-PP polymerization was stabilized inside the interlayer galleries with a catalytically benign environment. The MMT-borne catalyst, upon further activation by MAO, released fairly high activities for propylene polymerization. The effective intercalative polymerization ensured an efficient preparation of i-PP/MMT nanocomposite. A series of i-PP/MMT nanocomposites containing completely disordered MMT at a loading range of 1.0–6.7 wt% (TGA measurement residue at 600 °C) were obtained in high yields.

Keywords: i-PP/MMT nanocomposite; In situ polymerization; Metallocene catalysis

1. Introduction

Since the invention of nylon/montmorillonite (MMT) nanocomposites by Toyota researchers in 1980s [1], the study of MMT-reinforced polymer nanocomposites has been one of the most interesting research topics in the polymer science and materials community [2]. This is because the introduction of a few weight percent of nanometer-scale laminated silicate layers into a polymer matrix can drastically improve many of the polymer properties, such as modulus, strength, heat resistance, anti-flammability and anti-gas permeability, which are usually very difficult to access by traditional micrometer-scale inorganic fillers [3].

Polyolefins (PE, PP, etc.) are among the most interesting polymers deemed to benefit the most from the formation of nanocomposite with MMT due to their widespread applications [4]. In particular, isotactic polypropylene (i-PP), one of the most important class of polyolefins possessing many superior material properties in terms of mechanical, thermal, and processing requirements, has been asserted and partially realized with immense advantages for combining with MMT to produce high-performance polypropylene materials for advanced applications. However, i-PP, like other polyolefins, is of chemically nonpolar characteristic, which dictates its nearly complete immiscibility with inorganic MMT. This has raised serious problems for a direct polymer intercalation method (including melt and solution intercalations) to render effective nanoscopic

* Corresponding author. Tel./fax: +86 10 82611905.
E-mail address: jydong@iccas.ac.cn (J.-Y. Dong).
[1] Ph.D. candidate of the Graduate School, Chinese Academy of Sciences.

0032-3861/$ - see front matter © 2007 Elsevier Ltd. All rights reserved.
doi:10.1016/j.polymer.2007.08.046

dispersion of MMT in i-PP [5]. In order to successfully prepare i-PP and other polyolefin-based nanocomposites, several research groups have explored a so-called in situ polymerization method that avoids the inconvenient polymer intercalation process by allowing olefin monomers to grow to polymers in situ inside MMT interlayer gallery. As the unfavorable thermodynamic obstacle is bypassed, the in situ polymerization technique has been generally accepted as a convenient means to access polyolefin/MMT nanocomposites.

For in situ polymerization to prepare polyolefin/MMT nanocomposites, preparation efficiency is a very important criterion which is, however, often neglected in literatures. Differing from a conventional catalytic polymerization to produce net polyolefins where only yield or productivity is concerned, the preparation efficiency in the case of polyolefin/MMT nanocomposite has two-folds of meanings, which are integrated together to judge the effectiveness of the polymerization: one is still concerned with productivity, the other, however, is structure-related, dealing with the completeness of the nanoscopic dispersion (delamination) of MMT. In this context, in order to gain high preparation efficiency when a nanocomposite is targeted by a polymerization, it is logical to have the olefin polymerization catalyst species with full catalytic function stabilized inside MMT interlayer gallery to assure both the intercalative selectivity and the effectiveness of the subsequent olefin polymerization. O'Hare and coworkers ever took advantage of the ion-exchanged organic modification of MMT to intercalate a cationic metallocene species into MMT, which ensured an exclusive, stable existence of the polymerization species inside the interlayer gallery [6]. However, due to the inadequacy of the catalyst species to polymerize propylene to high polymer, their effort had only resulted in nanocomposites based on low molecular weight propylene oligomers. Most of the other reports, including our owns, have just described the MMT/catalyst incorporation process like a course of catalyst supporting on organically modified MMT using both heterogeneous Mg–$TiCl_4$ and homogeneous metallocene and non-metallocene catalysts [7–21]. Catalyst intercalation was mostly through physical absorption. Catalyst–MMT interaction was fragile. The intercalated catalyst species were easy to be removed from inside the interlayer gallery. In turn, the in situ olefin polymerization was of low intercalative selectivity, producing polyolefins to a limited extent in the interlayer galleries. Consequently, the nanoscopic exfoliation of MMT during the in situ polymerization was hardly complete. In fact, in many reported efforts (including our owns) of preparing PP/MMT nanocomposites using Mg–$TiCl_4$ catalyst and PE/MMT nanocomposites using (non-)metallocene catalyst, nanocomposites having well-exfoliated MMT could only be obtained at a maximum MMT loading well below 5.0 wt% [7–21]. Sun and Garcés reported a polymerization way to prepare PP/MMT nanocomposites using metallocene catalyst, claiming an almost exclusive intercalative polymerization [22]. However, the description was obscure. Jin et al. initiated an interesting solution by using a hydroxyl-functionalized surfactant to modify MMT, which implanted catalyst-anchoring reactive groups inside MMT interlayer gallery [23]. Unfortunately, they allowed $TiCl_4$ to directly react with hydroxyl group, causing the intercalated catalyst species to decay rapidly during ethylene polymerization.

2. Experimental part

2.1. Materials and instruments

All O_2- and moisture-sensitive manipulations were carried out in argon atmosphere using standard Schlenk techniques. AP-grade toluene was deoxygenated by argon purge before being refluxed over sodium for 48 h and distilled immediately before use. Methylaluminoxane (MAO, 1.4 mol/L in toluene) was purchased from Albermarle and used as received. *rac*-$Me_2Si(2\text{-Me-4-Ph-Ind})_2ZrCl_2$ was synthesized according to literature procedure [24]. Polymerization-grade propylene was supplied by Yanshan Petrochemical Co. of China. AP-grade diethylamine (Beijing Chemical Factory, China) and ethylene chlorohydrin (Beijing Xudong Chemical Factory, China) were used without further purification. 1-Chlorohexadecane was purchased from Aldrich and used as received. Hexadecyl trimethylammonium bromide surfactant was kindly provided by Professor Zongneng Qi in the same Institute. Pristine montmorillonite (Na–MMT) was produced by Qinghe Chemical Plant (China) with a cation-exchange capacity (CEC) of 100 mequiv./100 g.

The Al and Zr contents were determined by inductively coupled plasma atomic emission spectroscopy using an ICP-AES Leeman Labs Plasma-Spec ICP model 2.5. The specimens were prepared by stepwise treating of the MMTs with hydrogen fluoride acid, high-temperature ablation, and nitric acid again to transform the solid samples to clear solution ones. The melting temperatures of the polymers were determined by differential scanning calorimetry (DSC) using a Perkin–Elmer DSC-7 instrument controller at a heating rate of 10 °C min^{-1} under nitrogen atmosphere. Data were collected from the second scan curves. Wide-angle X-ray diffraction (WAXD) was performed on a D8 advance X-ray powder diffractometer (Bruker Co.) with Cu Kα radiation ($\lambda = 0.15406$ nm) at generator voltage of 40 kV and generator current of 40 mA. The scanned 2θ range was 1.5°–45°. The scanning rate was 2.0°/min. The interlayer spacing (d_{001}) of MMT was calculated in accordance with the Bragg equation: $2d \sin\theta = \lambda$. Small-angle X-ray diffraction (SAXD) was performed on a DMAX-2400 X-ray diffractometer with Cu Kα radiation ($\lambda = 0.15406$ nm) at generator voltage of 60 kV and generator current of 200 mA. The scanned 2θ range was 0.6°–10°. The scanning rate was 1.0°/min. Thermogravimetric analysis (TGA) was performed on a Perkin–Elmer TGA instrument under nitrogen atmosphere in a temperature range of 50–700 °C at a heating rate of 20 °C/min. Transmission electron microscopy (TEM) was carried out on a Jeol JEM2011 transmission electron microscope using an acceleration voltage of 200 kV. Solvent extraction of nanocomposite samples was carried out using xylene at refluxing temperature for 12 h. The molecular weight and molecular weight

distribution of the extracted polymers were determined by Gel Permeation Chromatography (GPC) using a Waters Alliance GPC 2000 instrument equipped with a refractive index (RI) detector and a set of u-Styragel HT columns of 106, 105, 104, and 103 pore sizes in series. The measurement was operated at 150 °C with 1,2,4-trichlorobenzene as the eluent with a flow rate of 0.7 mL/min. Narrow molecular weight PS samples were used as standards for calibration.

2.2. Synthesis of (2-hydroxylethyl) hexadecyl diethylammonium iodine surfactant

According to literature [25], 10.0 g (0.14 mol) diethylamine was heated to its boiling temperature in a 250 mL flask equipped with a condenser and a dropping funnel, then 8.4 g (0.11 mol) ethylene chlorohydrin was added in 1 h. Heating was continued for 8 h. The reaction mixture was cooled to ambient temperature, and water was added with constant shaking. The aqueous was extracted by EtOAc for three times. After a reduced-pressure distillation, β-diethylaminoethyl alcohol was obtained at 34 °C. Yield was 65%. ^{1}H NMR ($CDCl_3$, 300 MHz): $\delta = 1.03$ (t, 6H, $J = 7.2$ Hz), $\delta = 2.53$–2.60 (m, 6H), $\delta = 3.55$ (t, 2H, $J = 5.4$ Hz).

A mixture of 5.2 g (0.07 mol) β-diethylaminoethyl alcohol, 18.2 g (0.07 mol) 1-chlorohexadecane and 17.8 g (0.07 mol) iodine was stirred at refluxed acetone for 24 h. The reaction mixture was added into water. The aqueous was extracted by CH_2Cl_2 for three times. Solvent was removed partly in vacuum. The residue was purified by ethyl ether. The product was obtained as a pale yellow powder with a yield of 90%. ^{1}H NMR ($CDCl_3$, 300 MHz) $\delta = 0.88$ (t, 3H, $J = 6.3$ Hz), $\delta = 1.25$–1.41 (m, 32H), $\delta = 1.66$–1.74 (m, 2H), $\delta = 3.32$–3.38 (m, 2H), $\delta = 3.52$–3.60 (m, 6H), $\delta = 4.14$–4.18 (m, 2H). The structure of this surfactant was deduced as shown in Fig. 1(a).

2.3. Organic modification of Na–MMT

For the preparation of OMMT–$OH_{0.8}$, 5.0 g Na–MMT was dispersed in 500 mL distilled water while 2.0 g (4.0 mmol) of (2-hydroxylethyl) hexadecyl diethylammonium iodine was dissolved in 20 mL of anhydrous ethanol and 0.364 g (1.0 mmol) of hexadecyl trimethylammonium bromide in 10 mL of distilled water. The two salt solutions were individually added dropwise to the MMT suspension under vigorous stirring. The reaction was kept at 60 °C for 24 h. After stirring was stopped, the precipitate was collected by filtration and washed with hot water and ethanol several times until no I^- and Br^- could be detected by $AgNO_3$ solution (0.1 mol/L). The precipitate was dried in vacuum at 60 °C for 24 h and grounded to powder.

The preparation of OMMT–R and OMMT–OH followed the same procedure as that of OMMT–$OH_{0.8}$, only the mixed surfactant was replaced by individual surfactant alone.

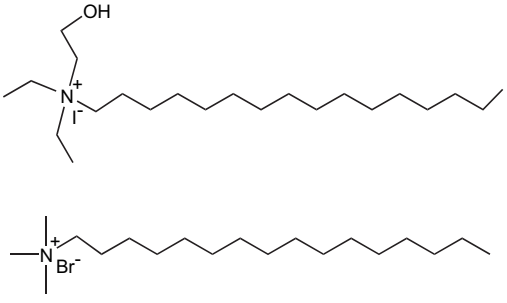

Fig. 1. Structures of the two surfactants: (a) (2-hydroxylethyl) hexadecyl diethylammonium iodine and (b) hexadecyl trimethylammonium bromide.

2.4. Preparation of the intercalated metallocene catalysts

In a typical reaction (OMMT–$OH_{0.8}$–C), to a 250 mL three-necked flask containing 3.0 g of OMMT–$OH_{0.8}$ (OH group content estimated at 1.0 mmol) was added 40 mL of toluene at 60 °C. The mixture was stirred for 1 h before 30 mL MAO (42.0 mmol) was introduced into the flask. After stirring for 7 h, 0.208 g of *rac*-Me_2Si(2-Me-4-Ph-Ind)$_2ZrCl_2$ was added. The reaction was allowed to proceed for 16 h. After decantation, the solid was washed with 50 mL toluene for five times and then dried in vacuum at 60 °C to obtain the OMMT–$OH_{0.8}$-intercalated *rac*-Me_2Si(2-Me-4-Ph-Ind)$_2ZrCl_2$ catalyst. The intercalated catalyst was denoted as OMMT–$OH_{0.8}$–C. Likewise, the OMMT–OH-intercalated *rac*-Me_2Si(2-Me-4-Ph-Ind)$_2ZrCl_2$ (OMMT–OH–C) and OMMT–R-intercalated *rac*-Me_2Si(2-Me-4-Ph-Ind)$_2ZrCl_2$ (OMMT–R–C) catalysts were prepared following the same procedure, only with OMMT–OH (OH group content estimated at 1.4 mmol) and OMMT–R, respectively.

2.5. Polymerization of propylene using the intercalated catalyst

The polymerization reactions were carried out with a Parr stainless-steel autoclave reactor equipped with a mechanical stirrer. In a typical reaction (run 1 in Table 3), 50 mL of toluene and 0.55 mL of MAO (1.4 mol/L in toluene) were introduced into the reactor which was pre-filled with propylene at 50 °C. The polymerization reaction was initiated by charging 0.10 g of the intercalated catalyst OMMT–$OH_{0.8}$–C. After polymerizing under a propylene pressure of 0.5 MPa for 0.5 h, the polymerization was quenched by acidified ethanol. The polymer product was collected by filtration and washed in turn with distilled water/ethanol mixture and acetone, and then dried under vacuum at 60 °C for 24 h.

3. Results and discussion

In this paper we discuss an efficient preparation of i-PP/MMT nanocomposites by in situ polymerization technique. The chemistry centers on a proper employment of a functional surfactant in the cation-exchanged organic modification of MMT and use of metallocene/MAO catalyst system for in situ propylene polymerization. Both the completeness of the nanoscopic dispersion (delamination) of MMT and the productivity of the polymerization are assured. Scheme 1 illustrates the overall reaction path.

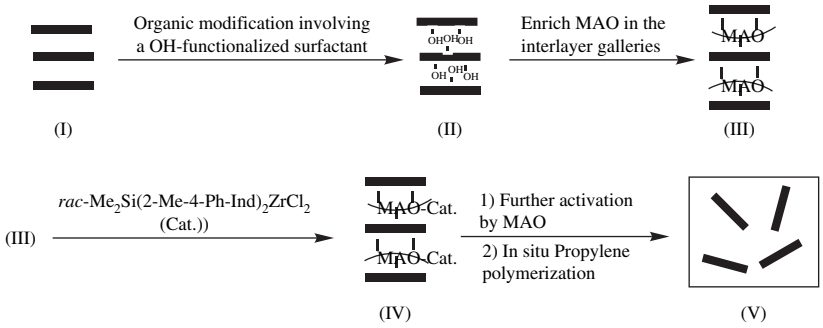

Scheme 1.

The partial involvement of the functional surfactant, (2-hydroxylethyl) hexadecyl diethylammonium iodine ($[(C_2H_5)_2(C_2H_4OH)(C_{16}H_{33})N]I$, chemical structure shown in Fig. 1(a)), in the organic modification of pristine Na−MMT (**I**) using the conventional hexadecyl trimethylammonium bromide surfactant ($[(CH_3)_3(C_{16}H_{33})N]Br$, chemical structure shown in Fig. 1(b)), results in an implantation of hydroxyl (OH) group in the interlayer gallery of MMT (OMMT) (**II**), which thus possesses a hydrophobic inner surface and enlarged gallery spacing. This intentionally introduced OH group serves as a catalyst-anchoring site to immobilize and amass MAO in the interlayer gallery. The MAO-enriched interlayer gallery (**III**) is ready to accept metallocene compound *rac*-Me_2Si[2-Me-4-Ph-Ind]$_2ZrCl_2$, one of the best C_2-symmetric zirconocenes for isospecific propylene polymerization, via complexation (**IV**). The MAO-covering of the inner gallery surface makes an excellent catalytically benign environment for the metallocene to fully exercise its catalytic function in the subsequent propylene polymerization. With both the intercalative selectivity and the effectiveness of the in situ polymerization assured, well-exfoliated MMT/i-PP nanocomposites (**V**) are expected at high preparation efficiency.

3.1. Preparation of organically modified MMTs (OMMTs) and OMMT-intercalated catalysts

Three organically modified MMTs (OMMTs) were prepared, one (OMMT−R) ion-exchanged solely by $[(CH_3)_3(C_{16}H_{33})N]Br$, the other two (OMMT−OH and OMMT−$OH_{0.8}$) by 100% $[(C_2H_5)_2(C_2H_4OH)(C_{16}H_{33})N]I$ and 80% $[(C_2H_5)_2(C_2H_4OH)(C_{16}H_{33})N]I$ (with 20% $[(CH_3)_3(C_{16}H_{33})N]Br$), respectively. The purpose of adding 20% $[(CH_3)_3(C_{16}H_{33})N]Br$ in MMT modification by $[(C_2H_5)_2(C_2H_4OH)(C_{16}H_{33})N]I$ is to reduce the concentration of OH group in the interlayer gallery of MMT so as to lower the negative effect of hetero atom O on the anchored metallocene catalyst. Characterization data of the three OMMTs are collected in Table 1, where a comparison is made with those of the pristine Na−MMT. WAXD patterns of the three OMMTs and Na−MMT are plotted in Fig. 2-A.

All ion-exchange reactions were successful, in spite of the slightly different TGA measurement residues at 600 °C, indicating that there might be deviations in the ion-exchange reaction using different surfactants. As illustrated in Fig. 2-A, distinct shifts of (001) diffraction peak of ordered silicate layers are observed for all OMMTs, OMMT−R at $2\theta = 4.48°$, OMMT−$OH_{0.8}$ at $2\theta = 4.18°$ and OMMT−OH at $2\theta = 3.92°$, compared to the pristine Na−MMT at $2\theta = 8.92°$. Accordingly, the d_{001} values are calculated at 1.98, 2.11, 2.25 and 0.98 nm for OMMT−R, OMMT−$OH_{0.8}$, OMMT−OH, and Na−MMT, respectively. These *d*-spacings (at around 2.0 nm) are sufficient for OMMTs to be intercalated effectively by MAO [30].

Table 1
Characterization data of the three OMMTs in comparison with Na−MMT

MMT	2θ (°)	$d_{(001)}$ (nm)	TGA measurement residue at 600 °C (wt%)
Na−MMT	8.92	0.98	≈100
OMMT−R	4.48	1.98	75.4
OMMT−$OH_{0.8}$	4.18	2.11	81.0
OMMT−OH	3.92	2.25	79.5

The combination of the metallocene catalyst, *rac*-Me_2Si(2-Me-4-Ph-Ind)$_2ZrCl_2$, with the three OMMTs was completed by the same procedure, i.e., firstly treating the OMMT with excessive MAO and then allowing the MAO-treated OMMT to react with the metallocene. The conditions for all reactions were of no difference. The obtained OMMT-based catalysts, OMMT−R/MAO/*rac*-Me_2Si(2-Me-4-Ph-Ind)$_2ZrCl_2$ (OMMT−R−C), OMMT−$OH_{0.8}$/MAO/*rac*-Me_2Si(2-Me-4-Ph-Ind)$_2ZrCl_2$ (OMMT−$OH_{0.8}$−C), and OMMT−OH/MAO/*rac*-Me_2Si(2-Me-4-Ph-Ind)$_2ZrCl_2$ (OMMT−OH−C), along with the pristine Na−MMT, were subjected to Zr and Al content measurements. These results, along with the WAXD characterization data, are given in Table 2 and in Fig. 2-B are plotted the WAXD patterns.

It is of no surprise that OMMT−R−C was found with both MAO and metallocene intercalations. The *d*-spacing increased from 1.98 nm in OMMT−R to 2.55 nm in OMMT−R−C. In our previous study, we also found that OMMT modified by ordinary, non-functionalized surfactant, e.g., $[(CH_3)_3(C_{16}H_{33})N]Br$, with an enlarged interlayer spacing at around 2 nm, could absorb MAO and metallocene for intercalation [16]. As the active surface hydroxyl group inherent in MMT is not rich, the intercalation of MAO into OMMT−R must be largely due to physical absorption. After all this OMMT composed of innumerous nanoscopic silicate layers possesses a very large surface area. The measured [Al] in OMMT−R−C is only 2−3 wt% lower than those in

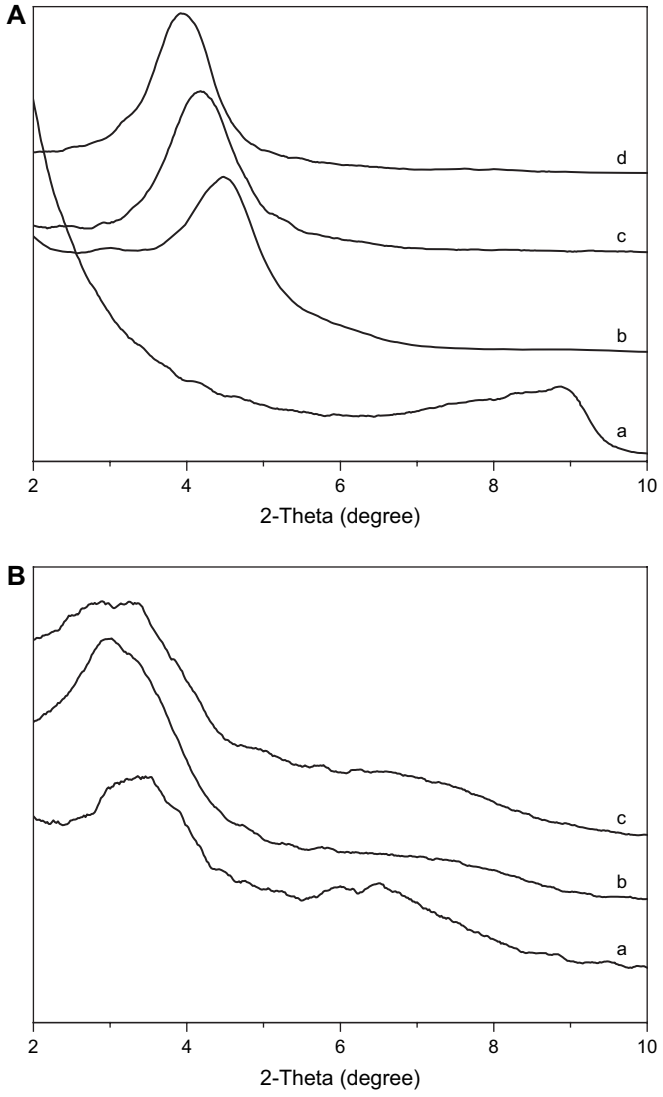

Fig. 2. WAXD patterns of (A) (a) pristine Na–MMT and three organically modified MMT, (b) OMMT–R, cation-exchanged with hexadecyl trimethylammonium bromide, (c) OMMT–$OH_{0.8}$, cation-exchanged with 80 wt% of (2-hydroxylethyl) hexadecyl diethylammonium iodine and 20 wt% of hexadecyl trimethylammonium bromide, and (d) OMMT–OH, cation-exchanged with (2-hydroxylethyl) hexadecyl diethylammonium iodine; and (B) three OMMT-intercalated catalysts: (a) OMMT–R/MAO-*rac*-Me_2Si(2-Me-4-Ph-Ind)$_2ZrCl_2$, (b) OMMT–$OH_{0.8}$/MAO-*rac*-Me_2Si(2-Me-4-Ph-Ind)$_2ZrCl_2$, and (c) OMMT–OH/MAO-*rac*-Me_2Si(2-Me-4-Ph-Ind)$_2ZrCl_2$.

Table 2
Characterization data of the three OMMT-supported catalysts, OMMT–R–C, OMMT–$OH_{0.8}$–C and OMMT–OH–C

MMT	[Zr] (wt%)	[Al] (wt%)	2θ (°)	$d_{(001)}$ (nm)
Na–MMT	≈0	2.63	8.92	0.98
OMMT–R–C	0.048	11.17	3.46	2.55
OMMT–$OH_{0.8}$–C	0.034	13.37	3.02	2.92
OMMT–OH–C	0.027	14.46	3.32	2.66

OMMT–$OH_{0.8}$–C and OMMT–OH–C. However, due to the lack of chemical bonding, such a combination of MAO with OMMT should not be conceived stable, i.e., it will not be able to withstand solvent leaching during olefin polymerization (in bulk or slurry reaction). At least partial detachment of MAO, along with the metallocene catalyst complexing with it, from the inner gallery of MMT is expectable in the in situ polymerization of nanocomposite preparation. In fact, we suspected that this was the reason that accounted for the low efficiency of PE/OMMT nanocomposites preparation using a [$(CH_3)_3(C_{16}H_{33})$N]Br-modified OMMT in our previous study [16].

On the other hand, the two hydroxyl-modified OMMTs, OMMT–$OH_{0.8}$ and OMMT–OH, were deemed to be able to stably shelter MAO as well as the complexing metallocene catalyst. The heterogenization of homogeneous metallocene catalysts on organic and inorganic substrates bearing hydroxyl functionality, e.g., silica gel and hydroxyl-functionalized PP granules, has been well studied and acknowledged to proceed via formation of covalent Al–O bond by surface hydroxyl group reaction with MAO [26–29]. In our current case, as both hydroxyl-modified OMMTs possessed an interlayer spacing larger than the size of MAO [30], which ensured successful MAO intercalation, the hydroxyl-MAO reaction could be presumed complete in consideration of the very high feeding ratios of [MAO] to [hydroxyl] (42/1 and 31/1 for OMMT–$OH_{0.8}$ and OMMT–OH, respectively). As shown in Table 2, the [Al] values of OMMT–$OH_{0.8}$–C (13.37 wt%) and OMMT–OH–C (14.46 wt%) are higher than that of OMMT–R–C (11.17 wt%), which is in accordance with the greater extents of the *d*-spacing increments for OMMT–$OH_{0.8}$–C and OMMT–OH–C as compared with OMMT–R–C from their respective prototypical OMMT–$OH_{0.8}$, OMMT–OH and OMMT–R. The complexing metallocene, *rac*-Me_2Si(2-Me-4-Ph-Ind)$_2ZrCl_2$, although showing no significant difference in amount among OMMT–$OH_{0.8}$–C, OMMT–OH–C and OMMT–R–C, is presumable to exist more stably inside the interlayer gallery in OMMT–$OH_{0.8}$–C and OMMT–OH–C.

It is also noted that all three OMMT-based catalysts, OMMT–$OH_{0.8}$–C, OMMT–OH–C and OMMT–R–C, show slightly broader (001) diffraction peaks in their WAXD patterns as compared with OMMTs. This implies that the intercalation of the catalyst components, MAO and metallocene, might not be very homogeneous from gallery to gallery.

3.2. In situ polymerization of propylene using OMMT–$OH_{0.8}$–C, OMMT–OH–C and OMMT–R–C and MAO

The results of propylene polymerization with the three OMMT-based catalysts, OMMT–$OH_{0.8}$–C, OMMT–OH–C and OMMT–R–C, are summarized in Table 3. The loading of MMT in each polymerization product was determined using the residual content at 600 °C in TGA measurement conducted in nitrogen atmosphere. In general, for OMMT–$OH_{0.8}$–C, catalyst activities per molar Zr per hour were in the range of 5.0×10^6–3.0×10^7 g PP/mol Zr per hour, depending on the [MAO]/[Zr] ratio used during polymerization, higher [MAO]/[Zr] ratio resulting in higher activity. Comparing runs 1 and 2 with runs 8 and 9, which adopted the same [MAO]/[Zr] ratios but with different catalysts, runs 1 and 2

Table 3
A summary of conditions[a] and results of propylene polymerization using OMMT−$OH_{0.8}$−C, OMMT−OH−C and OMMT−R−C and MAO

Run	Catalyst	[MAO]/[Zr] (mol/mol)	Cat. activity ($\times 10^7$ g PP/mol Zr per hour)	MMT (wt%)	T_m (°C)	T_{onset} (°C)
1	OMMT−$OH_{0.8}$−C	2000	0.59	6.69	157.4	383.2
2	OMMT−$OH_{0.8}$−C	4000	0.82	5.78	157.4	425.6
3[b]	OMMT−$OH_{0.8}$−C	6000	2.02	2.11	157.6	429.9
4	OMMT−$OH_{0.8}$−C	6000	1.61	1.90	157.4	437.8
5	OMMT−$OH_{0.8}$−C	8000	2.75	1.03	157.8	424.5
6	OMMT−OH−C	2000	–	–	–	–
7	OMMT−OH−C	8000	0.88	4.51	158.1	420.3
8[c]	OMMT−R−C	2000	0.93	4.30	156.4	394.1
9[c]	OMMT−R−C	4000	1.22	1.00	156.6	417.3

[a] Other conditions: 0.4 MPa propylene, 50 mL toluene, 50 °C, polymerization time = 30 min.
[b] Polymerization time = 20 min.
[c] Toluene (100 mL).

with OMMT−$OH_{0.8}$−C and runs 8 and 9 with OMMT−R−C, it is noteworthy that OMMT−$OH_{0.8}$−C is only slightly inferior to OMMT−R−C in catalyst activity, despite the fact that it encloses a quite large amount of O-containing molecules. However, it is recognized that both polymerization reactions with OMMT−OH−C (runs 6 and 7) were of much lower catalyst activities. Comparing runs 3 and 4, it is noted that, with OMMT−$OH_{0.8}$−C, catalyst activity decreased with polymerization time. This adds complexity in controlling nanocomposite composition by simple polymerization time adjustment.

Hybrids of i-PP/OMMT containing 1.03, 1.90, 2.11, 5.78, and 6.69 wt% of MMT (TGA measurement residue at 600 °C) (runs 1−5 in Table 3) were obtained with OMMT−$OH_{0.8}$−C. These polymers were cold-pressed into compact, plate-form specimens for WAXD examination. In Fig. 3-A are illustrated WAXD patterns of the five samples. No (001) diffraction peak of ordered silicate layer parallel stack is discerned in any of them, irrespective of the MMT loading in the sample, indicating roughly a well-exfoliation of MMT in i-PP matrix for each hybrid. To confirm these results, three of the samples containing 6.69, 5.78, and 1.90 wt% of MMT (runs 1, 2, and 4 in Table 3) were subjected to SAXD examination to specify the low angle range for any diffraction signal that might be missed by WAXD. Fig. 3-B plots the three SAXD patterns. The results are consistent with those of WAXD; no more signals appearing in the 2θ range of 1°−10°, even for the two high MMT-loading samples from runs 1 and 2.

Fig. 4 shows two TEM images of a hybrid containing 6.69 wt% of MMT (run 1 in Table 3). Both pictures were obtained on the same specimen but taken at different spots. The elegantly dispersed nanoscopic silicate layers (mostly <5 nm in thickness) of MMT are clearly discerned.

On the other hand, MMT dispersion in hybrids prepared by OMMT−R−C is highly dependent on MMT loading. Fig. 5 illustrates WAXD patterns of two i-PP/OMMT samples resulting from OMMT−R−C (runs 8 and 9 in Table 3). Only a very weak and broad signal was detected at around $2\theta = 6.30°$ for the hybrid containing 1.00 wt% of MMT. However, at

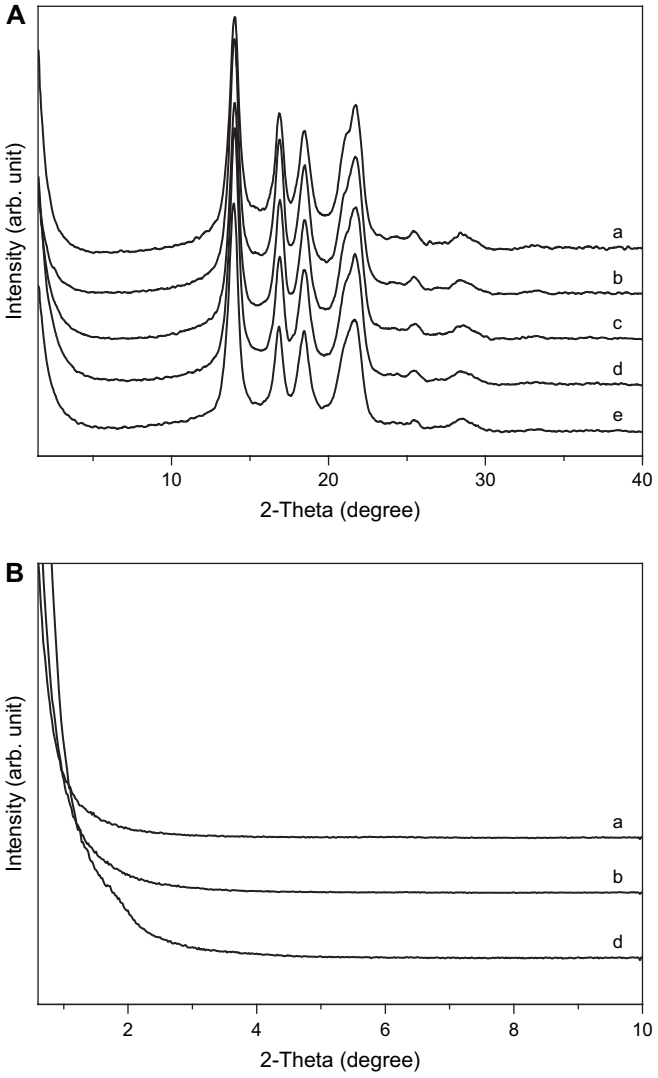

Fig. 3. Powder (A) WAXD and (B) SAXD patterns of i-PP/OMMT−$OH_{0.8}$ nanocomposites containing (a) 6.69, (b) 5.78, (c) 2.11, (d) 1.90, and (e) 1.03 wt% of inorganic MMT based on the calculation of percentage of residue at 600 °C in TGA curve (runs 1−5 in Table 3).

$2\theta = 6.25°$, corresponding to an interlayer distance of 1.41 nm, a relatively strong diffraction peak due to poorly dispersed parallel stacks of MMT was clearly observed for hybrid containing 4.30 wt% of MMT. This peak appears at a different 2θ angle than the starting OMMT−R as well as OMMT−R−C, which may be because of the transformation of the aggregation mode of the surfactant moiety from bilayer to monolayer arrangement in the interlayer gallery during the polymerization process or in the specimen preparation step. Overall, these results indicate that, with OMMT−R−C, MMT cannot be effectively exfoliated in polymerization. In other words, the nanocomposite preparation efficiency is low.

Hybrids prepared by OMMT−$OH_{0.8}$−C as well as other two OMMT-based catalysts all possess a highly isotactic polypropylene matrix, which are evidenced by the generally high melting points measured by DSC. The WAXD patterns also reveal that the i-PP matrix crystallized in α-form, as they show diffraction peaks at $2\theta = 13.9$, 16,8, 18.4 and 21.7

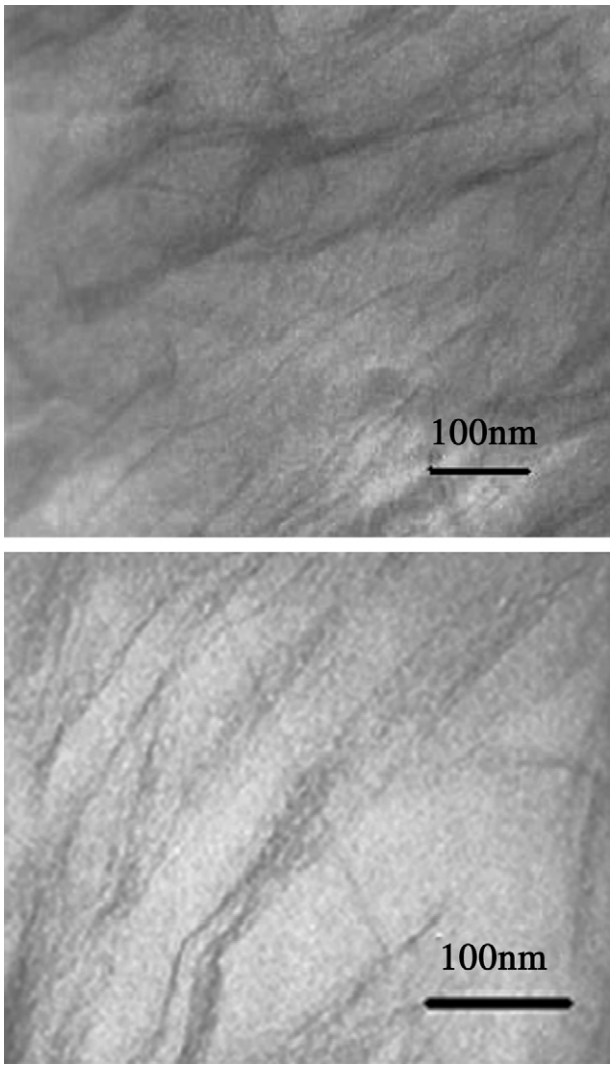

Fig. 4. TEM images of i-PP/OMMT−$OH_{0.8}$ nanocomposite containing 6.69 wt% of inorganic MMT based on the calculation of percentage of residue at 600 °C in TGA curve (run 1 in Table 3).

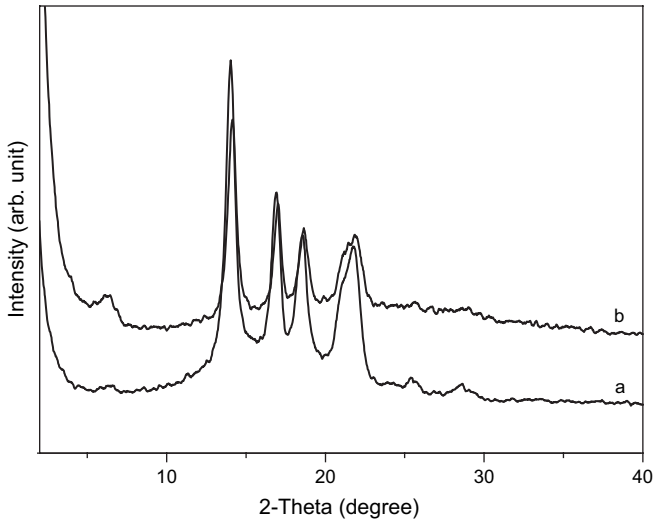

Fig. 5. Powder WAXD patterns of i-PP/OMMT−R nanocomposites containing (a) 1.00 and (b) 4.30 wt% of inorganic MMT based on the calculation of percentage of residue at 600 °C in TGA curve (runs 8 and 9 in Table 3).

Table 4
Matrix molecular weight and molecular weight distribution of nanocomposites prepared by OMMT−$OH_{0.8}$−C

Entry in Table 3	M_n ($\times 10^5$)	M_w ($\times 10^5$)	M_w/M_n
2	2.2	6.8	3.18
4	1.1	4.7	4.42
5	1.2	4.1	3.34

corresponding to the crystallite planes of (110), (040), (130) and (111). To determine the molecular weight of the isotactic polypropylene matrix, solvent extraction was carried out using xylene at refluxing temperature on three nanocomposite samples prepared by OMMT−$OH_{0.8}$−C (runs 2, 4 and 5 in Table 3). The extracted polymer samples were subjected to GPC measurement. The results are summarized in Table 4, showing that the polymer matrixes are of high molecular weight.

The thermogravimetric analysis data (T_{onset}) indicate that the exfoliated nanocomposites generally possess better thermal stability, due to the laminated layers of MMT acting as physical barriers and deterring the thermal transmission in the polymer matrix. This was deduced from comparing runs 2−5 with runs 8 and 9. The exceptionally low T_{onset} for run 1 might be due to the decomposition of surfactant that accelerated the thermal decomposition of the PP matrix.

4. Conclusion

In summary, with the combined use of a functional surfactant for MMT organic modification and a metallocene catalyst system for isospecific propylene polymerization, both the intercalative selectivity and the effectiveness of the in situ propylene polymerization were assured, which have led to an efficient preparation of i-PP/MMT nanocomposites using the in situ polymerization technique. The use of a mixed surfactant containing 80% OH-functionalized (2-hydroxylethyl) hexadecyl diethylammonium iodine surfactant and 20% conventional hexadecyl trimethylammonium bromide surfactant in the cation-exchanged organic modification of MMT not only provided catalyst-anchoring reactive sites to facilitate the stabilization of catalyst species in MMT interlayer gallery but also helped to create a catalytically benign environment for the intercalated metallocene to fully exercise its catalytic function in polymerization. The metallocene catalyst *rac*-Me_2Si[2-Me-4-Ph-Ind]$_2ZrCl_2$ confined in the interlayer galleries of MMT released fairly high activity in the in situ propylene polymerization, which ensured both the nanoscopic dispersion (delamination) of MMT and the productivity of the polymerization. Consequently, a series of i-PP/MMT nanocomposites containing disordered MMT at a loading range of 1.0−6.7 wt% (TGA measurement residue at 600 °C) were prepared in high yield.

Acknowledgement

Financial supports from the National Science Foundation of China (Grant Nos. 50373048 and 50573081) and Ministry of

Science and Technology of China (“973” project, G2003 CB615600) are gratefully acknowledged.

References

[1] Okada A, Kawasumi M, Kurauchi T, Kamigaito O. Polym Prepr (Am Chem Soc Div Polym Chem) 1987;28:447–8.
[2] Sinha Ray S, Okamoto M. Prog Polym Sci 2003;28:1539–41.
[3] Usuki A, Hasegawa N, Kato M. Adv Polym Sci 2005;179:135–95.
[4] Galli P, Vecellio G. J Polym Sci Part A Polym Chem 2004;42:396–415.
[5] Manias E, Wu TL, Strawhecker K. Chem Mater 2001;13:3516–23.
[6] Tudor J, Willington L, O’Hare D, Royan B. Chem Commun 1996; 2031–2.
[7] Hwu JM, Jiang GJ. J Appl Polym Sci 2005;95:1228–36.
[8] Ma JS, Qi ZN, Hu YL. J Appl Polym Sci 2001;82:3611–7.
[9] Weiss K, Wirth PC, Hofmann M, Botzenhardt S, Lang H, Brüning K, et al. J Mol Catal A Chem 2002;182–183:143–9.
[10] He AH, Hu HQ, Huang YJ, Dong JY, Han CC. Macromol Rapid Commun 2004;25:2008–13.
[11] He AH, Wang LM, Li JX, Dong JY, Han CC. Polymer 2006;47:1767–71.
[12] Yang KF, Huang YJ, Dong JY. Chin Sci Bull 2007;52:181–7.
[13] Ray S, Galgali G, Lele A, Sivaram S. J Polym Sci Part A Polym Chem 2005;43:304–18.
[14] Bergman JS, Chen H, Giannelis EP, Thomas MG, Coates GW. Chem Commun 1999;2179–80.
[15] Zhang XQ, Yang F, Zhao HC. US Patent 6,613,711 B2; 2003.
[16] Huang YJ, Yang KF, Dong JY. Macromol Rapid Commun 2006;27:1278–83.
[17] Jeong DW, Hong DS, Cho HY, Woo SI. J Mol Catal A Chem 2003;206:205–11.
[18] Lee DH, Kim HS, Yoon KB, Min KE, Seo KH, Noh SK. Sci Technol Adv Mater 2005;6:457–62.
[19] Alexandre M, Dubois P, Sun T, Garces JM, Jérôme R. Polymer 2002;43:2123–32.
[20] Liu CB, Tang T, Wang D, Huang BT. J Polym Sci Part A Polym Chem 2003;41:2187–96.
[21] Liu CB, Tang T, Zhao ZF, Huang BT. J Polym Sci Part A Polym Chem 2002;40:1892–8.
[22] Sun T, Garcés J. Adv Mater 2002;14:128–30.
[23] Jin YH, Park HJ, Im SS, Kwak SY, Kwak SJ. Macromol Rapid Commun 2002;23:135–40.
[24] Spaleck W, Küber F, Winter A, Rohrmann J, Bachmann B, Antberg M, et al. Organometallics 1994;13:954–63.
[25] Hartman WW. Org Syn Coll 1943;2:183.
[26] Kaminsky W, Funck A, Wiemann K. Macromol Symp 2006;239:1–6.
[27] Li KT, Kao YT. J Appl Polym Sci 2006;101:2573–80.
[28] Fink G, Steinmetz B, Zechlin J, Przybyla C, Tesche B. Chem Rev 2000;100:1377–90.
[29] Liu JG, Dong JY, Cui NN, Hu YL. Macromolecules 2004;37:6275–82.
[30] Sano T, Doi K, Hagimoto H, Wang Z, Uozumi T, Soga K. Chem Commun 1999;733–4.